The EMBO Journal Vol.18 No.5 pp.1303–1308, 1999

Encoding of Ca^{2+} signals by differential expression of IP_3 receptor subtypes

Tomoya Miyakawa, Akito Maeda[1], Toshiko Yamazawa, Kenzo Hirose, Tomohiro Kurosaki[1] and Masamitsu Iino[2]

Department of Pharmacology, Faculty of Medicine, The University of Tokyo, CREST, Japan Science and Technology Corporation, Bunkyo-ku, Tokyo 113 and [1]Akito Maeda, Tomohiro Kurosaki, Department of Molecular Genetics, Institute for Liver Research, Kansai Medical University, Moriguchi 570, Japan

[2]Corresponding author
e-mail: iino@m.u-tokyo.ac.jp

Inositol 1,4,5-trisphosphate (IP_3) plays a key role in Ca^{2+} signalling, which exhibits a variety of spatio-temporal patterns that control important cell functions. Multiple subtypes of IP_3 receptors (IP_3R-1, -2 and -3) are expressed in a tissue- and development-specific manner and form heterotetrameric channels through which stored Ca^{2+} is released, but the physiological significance of the differential expression of IP_3R subtypes is not known. We have studied the Ca^{2+}-signalling mechanism in genetically engineered B cells that express either a single or a combination of IP_3R subtypes, and show that Ca^{2+}-signalling patterns depend on the IP_3R subtypes, which differ significantly in their response to agonists, i.e. IP_3, Ca^{2+} and ATP. IP_3R-2 is the most sensitive to IP_3 and is required for the long lasting, regular Ca^{2+} oscillations that occur upon activation of B-cell receptors. IP_3R-1 is highly sensitive to ATP and mediates less regular Ca^{2+} oscillations. IP_3R-3 is the least sensitive to IP_3 and Ca^{2+}, and tends to generate monophasic Ca^{2+} transients. Furthermore, we show for the first time functional interactions between coexpressed subtypes. Our results demonstrate that differential expression of IP_3R subtypes helps to encode IP_3-mediated Ca^{2+} signalling.

Keywords: calcium/calcium imaging/gene targeting/ inositol 1,4,5-trisphosphate/IP_3 receptor

Introduction

Inositol 1,4,5-trisphosphate (IP_3)-mediated Ca^{2+} signalling controls important cell functions, such as contraction, secretion, gene expression and synaptic plasticity (Berridge, 1993). It is remarkable that a molecule as simple as Ca^{2+} can control a multitude of cellular functions with specificity, and the variety of spatio-temporal patterns of Ca^{2+} signalling has been implicated in its versatility. Indeed, the frequency of periodic increases in intracellular Ca^{2+} concentration (Ca^{2+} oscillation) has been shown to be important for the efficiency and specificity of gene expression (Dolmetsch *et al*., 1998; Li *et al*., 1998), and protein kinase activation (De Koninck and Schulman, 1998). However, it is not known how cells generate specific Ca^{2+}-signalling patterns. Multiple subtypes of IP_3 receptors (IP_3R-1, -2 and -3) are expressed in a tissue- and development-specific manner (Newton *et al*., 1994; Wojcikiewicz, 1995; Dent *et al*., 1996) and form heterotetrameric channels (Joseph *et al*., 1995; Monkawa *et al*., 1995). Therefore, the complex expression pattern of IP_3R subtypes may be responsible for the generation of cell type-specific Ca^{2+} signalling. Recent studies of individual IP_3R subtypes incorporated into lipid bilayers have suggested functional differences (Hagar *et al*., 1998; Ramos-Franco *et al*., 1998). However, the properties of IP_3R subtypes have not been systematically compared under equivalent cellular conditions and it has not been demonstrated whether or not there are IP_3R subtype-specific Ca^{2+}-signalling patterns. We have studied the physiological significance of the differential expression of IP_3R subtypes in conjunction with Ca^{2+}-signalling patterns, using genetically engineered B cells that express either a single or a combination of IP_3R subtypes. Our results show that temporal patterns of Ca^{2+} signals depend critically on the expressed set of IP_3R subtypes, which differ significantly in their response to intracellular agonists, i.e. IP_3, Ca^{2+} and ATP. Furthermore, we present the first evidence that coexpressed IP_3R subtypes make functional interactions. Thus, Ca^{2+}-signalling patterns can be encoded by differential expression of IP_3R subtypes.

Results and discussion

Ca^{2+} signalling in cells expressing a single IP_3R subtype

Three subtypes of IP_3Rs are expressed in DT40 B cells (Sugawara *et al*., 1997). Using an homologous recombination technique, we disrupted either one, two or all three IP_3R subtype genes (Sugawara *et al*., 1997) (Figure 1A). The loss of protein expression of IP_3R-1 and IP_3R-2 was confirmed in the cells with the respective gene disruption using antibodies specific to each IP_3R subtype (Figure 1B).

Ligation of the B-cell receptor (BCR) with an anti-BCR antibody induces the production of IP_3 via phosphorylation of phospholipase Cγ, resulting in mobilization of the Ca^{2+} stores in DT40 B cells (Kurosaki, 1997). We studied the changes in intracellular Ca^{2+} concentration ($[Ca^{2+}]_i$) upon activation of BCR in Fura-2-loaded DT40 cells with various combinations of IP_3R subtype expression. Ca^{2+} oscillations were observed in wild-type cells, which decayed in ~2–3 min and resumed thereafter, lasting for 1 h or longer (Figure 2A). Strikingly, mutant cells expressing only IP_3R-2 showed Ca^{2+} oscillations which were more regular and robust than those observed in wild-type cells (Figure 2C). On the other hand, mutant cells expressing either IP_3R-1 or IP_3R-3 showed only monophasic Ca^{2+} transient or very rapidly damped Ca^{2+} oscillations (Figure 2B, D and E). In ~75% of the mutant

cells expressing IP_3R-1, irregular Ca^{2+} oscillations with attenuated amplitude resumed subsequently (Figure 2B, lower panel). A delayed Ca^{2+} response was rarely observed (<1/h) in cells expressing IP_3R-3. Mutant cells expressing IP_3R-2 along with either IP_3R-1 or -3 also showed robust Ca^{2+} oscillations, while those expressing both IP_3R-1 and -3 but not IP_3R-2 showed a Ca^{2+} response similar to that of cells expressing only IP_3R-1 (data not shown). Thus, expression of IP_3R-2 is required for efficient generation of Ca^{2+} oscillations in DT40 cells. Disruption of IP_3R genes did not significantly affect cell-surface expression of the BCR (Sugawara *et al*., 1997). Furthermore, the subtype-specific Ca^{2+}-signalling patterns were not altered when the antibody concentration was varied between 0.01 and 10 μg/ml, although the fraction of cells responding changed (data not shown). These results indicate that the characteristic Ca^{2+}-signalling patterns were determined not by the stimulus intensity but by the expressed subtypes of IP_3Rs.

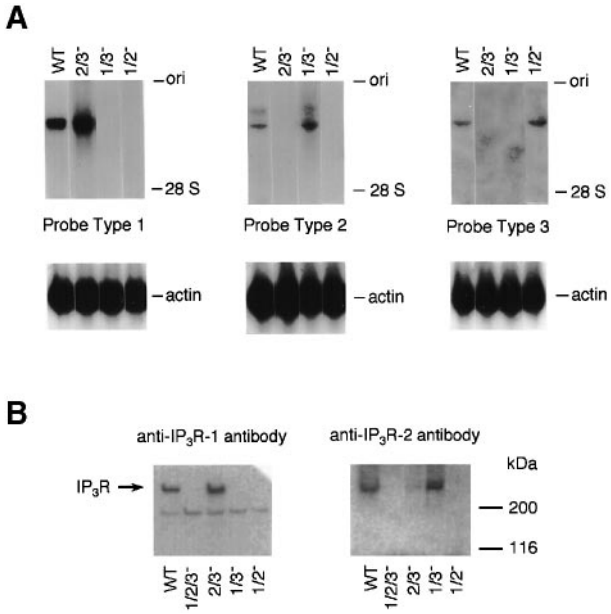

Fig. 1. Generation of DT40 cells expressing a single IP_3R subtype. (**A**) Northern analysis of wild-type (WT) and mutant DT40 cells with disruption of two of the three IP_3R genes (e.g. IP_3R-2 and -3 genes were disrupted in cells marked with $2/3^-$). (**B**) Western blot analysis after immunoprecipitation confirming the loss of expression of IP_3R-1 and -2 when the respective genes were disrupted using a polyclonal antibody against either IP_3R-1 or IP_3R-2 (see Materials and methods). In cells marked with $1/2/3^-$, all three IP_3R subtype genes were disrupted.

Luminal Ca^{2+} monitoring to study IP_3R functions

To investigate further the subtype-specific Ca^{2+}-signalling mechanism, we examined the functional differences between the subtypes using luminal Ca^{2+} monitoring (Hofer and Machen, 1993; Hirose and Iino, 1994; Hajnóczky and Thomas, 1997). Cells were loaded with Furaptra, a low-affinity fluorescent Ca^{2+} indicator (Raju *et al*., 1989) (Figure 3A and B). The fluorescence remaining after permeabilization of the cell membrane with β-escin was distributed in the extranuclear region in accordance with its localization within the endoplasmic reticulum (Figure 3C). Indeed, the luminal Ca^{2+} concentration increased with activation of the Ca^{2+} pump and declined upon application of IP_3 (Figure 3D). Thus, we measured the unidirectional flux of Ca^{2+} through the IP_3Rs by continuous monitoring of luminal Ca^{2+} concentration after withdrawing Mg^{2+}-ATP to disable Ca^{2+}-pump activity. No Ca^{2+} release was observed upon application of caffeine, an activator of the ryanodine receptor (Figure 3E); nor was IP_3-induced Ca^{2+} release observed in cells in which all the three IP_3R genes were disrupted (Sugawara *et al*., 1997) (Figure 3F). Therefore, the three IP_3R subtypes account for all the Ca^{2+}-release channels expressed in this cell line.

The time course of Ca^{2+} release did not follow a single exponential as reported in many other cell types (Figure 3G). However, as was the case in smooth muscle cells (Hirose and Iino, 1994), the time course of Ca^{2+} release at lower IP_3 concentrations became superimposable with that at 10 μM IP_3 if normalized to the half time ($t_{1/2}$). This indicates that the level of activation of the IP_3Rs can be quantitatively compared by the initial rate of Ca^{2+} release, which we estimated by fitting an exponential curve to the initial part of the Ca^{2+} decay signal. Thus, the

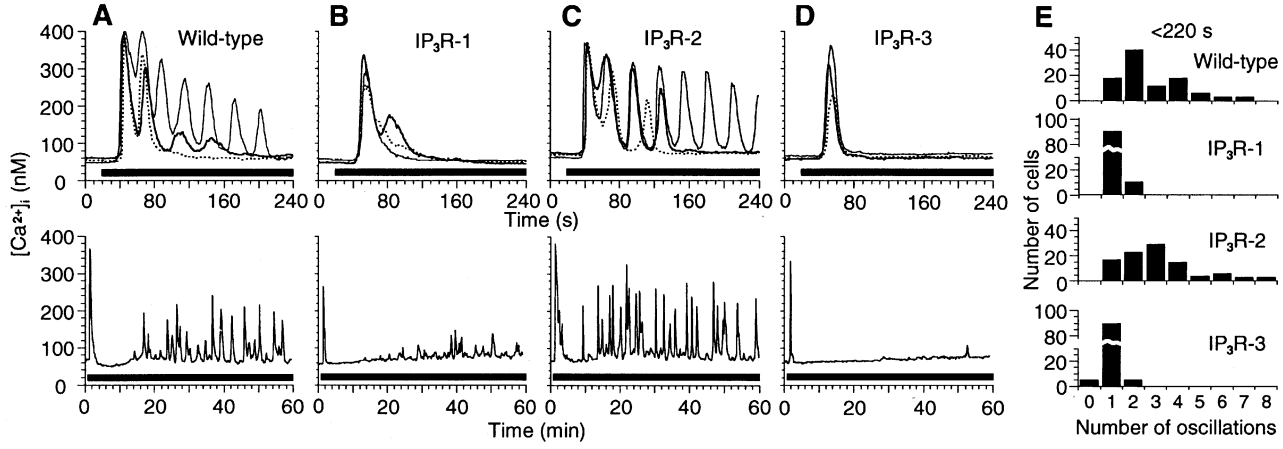

Fig. 2. Ca^{2+} signalling in DT40 cells expressing a single IP_3R subtype upon BCR stimulation. (**A**–**D**) Ca^{2+} response in single cells upon ligation of BCR with anti-BCR antibody (1 μg/ml). Wild-type cells (A) and mutant cells expressing either IP_3R-1 (B), -2 (C) or -3 (D). At the antibody concentration used, 95% of the cells exhibited at least one Ca^{2+} transient within 220 s in all cell types. Upper and lower traces show representative traces of the early and late responses, respectively. Antibody was applied as indicated by the horizontal bars below the traces. (**E**) Histogram for the number of Ca^{2+} oscillations within 220 s of BCR stimulation (100 cells from three cultures in each cell type).

combined use of luminal Ca^{2+} monitoring and genetically engineered cells provided us with a unique system to study quantitatively the properties of IP_3R subtypes expressed individually or along with other subtypes in an identical cellular context.

Agonist sensitivities of individual IP_3R subtypes

We first analysed the IP_3-induced Ca^{2+} release in cells expressing a single IP_3R subtype. Although IP_3 (10 μM) induced rapid Ca^{2+} release in wild-type cells in the absence of ATP, the rate of Ca^{2+} release was extremely low in IP_3R-1-expressing cells (Figure 4A). It has been shown that IP_3R activity is enhanced by ATP in a hydrolysis-independent manner in smooth muscle and cerebellar preparations (Iino, 1991; Bezprozvanny and Ehrlich, 1993; Missiaen *et al*., 1998) in which the dominant IP_3R subtype is IP_3R-1 (Newton *et al*., 1994; Wojcikiewicz, 1995). Indeed, the rate of Ca^{2+} release was enhanced by ATP (in the absence of Mg^{2+}) in IP_3R-1-expressing cells with an EC_{50} of 0.39 mM, while no effect was observed in wild-type cells (Figure 4A and B). The effect of ATP on IP_3R-1 was mimicked by β,γ-methylene ATP, a nonhydrolysable ATP analogue (data not shown). A less significant effect of ATP on IP_3R-3 was observed, whereas Ca^{2+} release via IP_3R-2 was insensitive to ATP (Figure 4C).

We then studied the IP_3 concentration dependence of Ca^{2+} release (Figure 5A). The IP_3 sensitivity was in the order of IP_3R-2 > IP_3R-1 > IP_3R-3; the EC_{50} obtained by hyperbolic fitting (see the legend to Figure 5) being 0.35, 4.7 and 18.6 μM, respectively. The extrapolated values of the maximal rate of Ca^{2+} release (r_{max}) were 0.063, 0.129 and 0.108 s^{-1} in cells expressing IP_3R-1, -2 and -3, respectively. Thus r_{max} was comparable within a factor of two among DT40 clones expressing different IP_3R subtypes.

IP_3R activity has been shown to be dependent on the cytoplasmic Ca^{2+} concentration in a biphasic manner in many cell types (Iino, 1990; Bezprozvanny *et al*., 1991; Finch *et al*., 1991). This property has been thought to

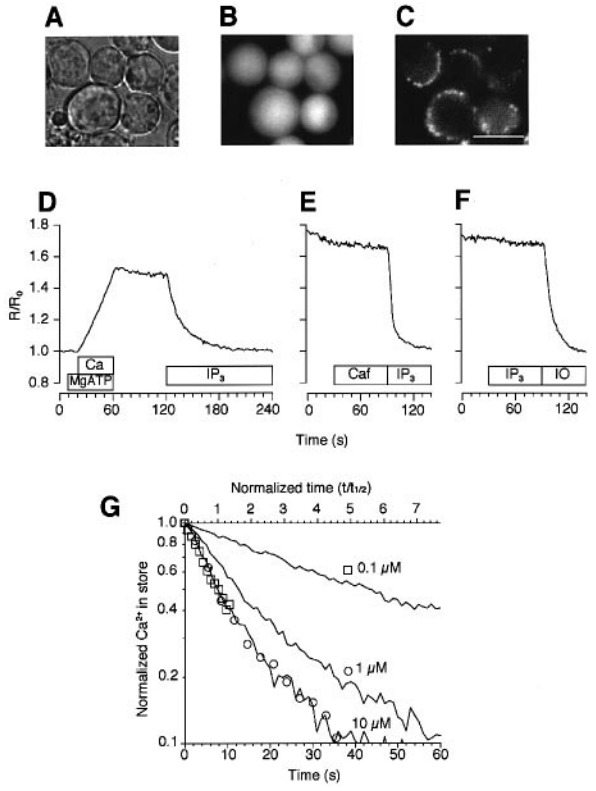

Fig. 3. Luminal Ca^{2+} measurement in single cells. Single DT40 cells under transmitted light (**A**), fluorescence intensity at 380 nm after loading with Furaptra (**B**) and after subsequent permeabilization with β-escin (**C**). The central region of the cells is occupied by the nucleus. Scale bar, 10 μm. (**D**) Change in fluorescence intensity ratio (R) normalized by R_0 in the Ca^{2+}-depleted state during Ca^{2+} loading (400 nM Ca^{2+} plus 0.5 mM Mg^{2+}-ATP), washout of Mg^{2+}-ATP and Ca^{2+} release (3 μM IP_3 at 100 nM Ca^{2+}). The Ca^{2+} loading–release cycles could be repeated several times in the same cells. (**E**) Caffeine (Caf; 20 mM) failed to induce Ca^{2+} release, but subsequent application of IP_3 (10 μM) released Ca^{2+}. (**F**) IP_3 (10 μM) failed to induce Ca^{2+} release in cells in which all three IP_3R subtype genes were disrupted, although subsequent application of ionomycin (IO; 1 μM) induced Ca^{2+} release. (**G**) Normalized time course of Ca^{2+} release at different IP_3 concentrations. Continuous lines, time courses of Ca^{2+} release at 0.1, 1 and 10 μM IP_3 (lower abscissa). Time course at 0.1 μM (□), 1 μM (○) and 10 μM (continuous line) was normalized to the half-time ($t_{1/2}$) of Ca^{2+} release for each IP_3 concentration (upper abscissa).

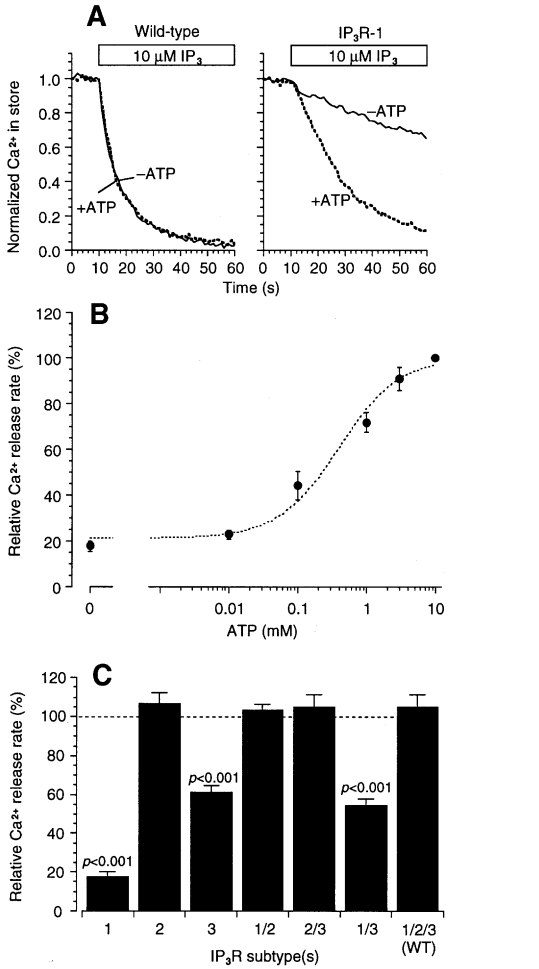

Fig. 4. ATP dependence of IP_3-induced Ca^{2+} release. (**A**) ATP (5 mM) had virtually no effect in wild-type cells, but greatly enhanced IP_3-induced Ca^{2+} release in IP_3R-1 expressing cells. (**B**) ATP dependence of the rate of IP_3-induced Ca^{2+} release in IP_3R-1-expressing cells. (**C**) Percentage of the rate of Ca^{2+} release (10 μM IP_3, 300 nM Ca^{2+}) in the absence of ATP compared with that in the presence of 10 mM ATP in cells expressing various IP_3R subtypes. Results are the mean ± SEM for four experiments.

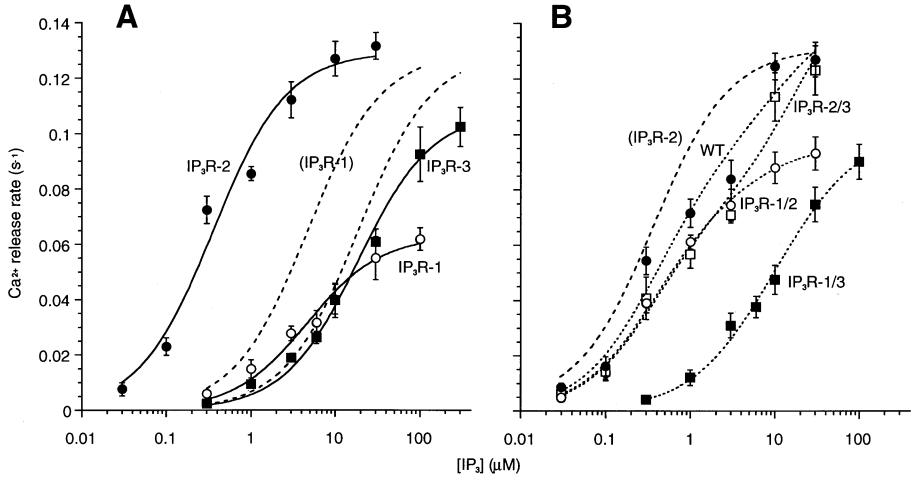

Fig. 5. IP_3-concentration dependence of Ca^{2+} release. (**A**) Ca^{2+} release in cells expressing a single IP_3R subtype. Continuous curves represent the best fit hyperbolic equations, $r_{max,i}/(1 + EC_{50,i}/[IP_3])$ for subtype *i*. For IP_3R-1 and -3, the fitted curves were scaled upward (dashed curves) so that r_{max} was the same as that of IP_3R-2 for the ease of comparison of EC_{50}s. (**B**) Ca^{2+} release rate in cells expressing multiple IP_3R subtypes. Dashed curve shows the fitted curve for IP_3R-2 in (A). Dotted curves show summation of the fitted equations, $\Sigma\{f_i \cdot r_{max,i}/(1 + EC_{50,i}/[IP_3])\}$, for $i = 1, 2, 3$. When subtype *i* was not expressed f_i was set to zero. Sets of (f_1, f_2, f_3) obtained by a least-squares method were as follows: (0.32, 0.60, 0), (0, 0.57, 0.82), (0.71, 0, 0.51), (0.37, 0.70, 0.31) for cells expressing IP_3R subtypes 1/2, 2/3, 1/3 and 1/2/3 (wild type), respectively. Ca^{2+} concentration was 100 nM. Ca^{2+} release via IP_3R-1 was studied in the presence of 5 mM ATP. Results are the mean ± SEM for 4–5 experiments.

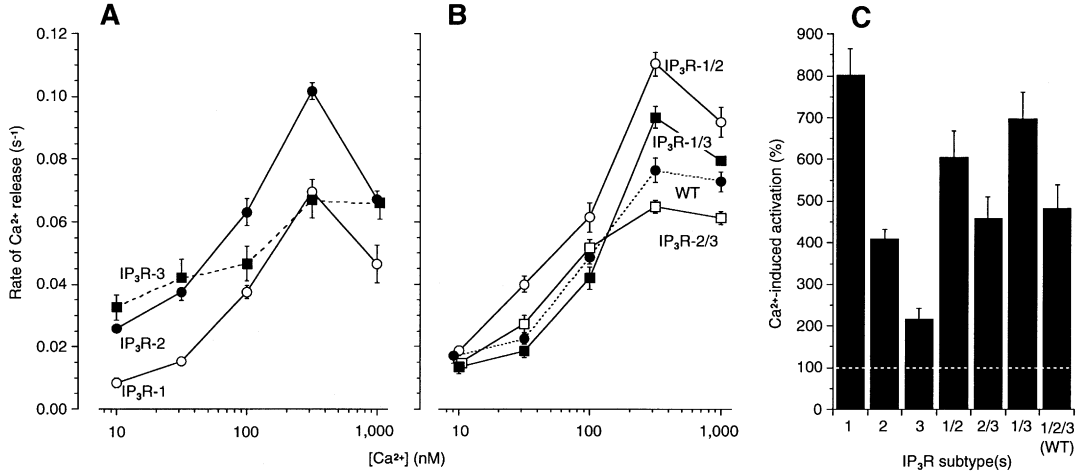

Fig. 6. Ca^{2+}-concentration dependence of IP_3-induced Ca^{2+} release. (**A**) Ca^{2+} release in cells expressing a single IP_3R subtype. (**B**) Ca^{2+} release in cells expressing multiple IP_3R subtypes. (**C**) Ca^{2+}-mediated activation of IP_3-induced Ca^{2+} release. Percentage increase of the Ca^{2+}-release rate at 300 nM Ca^{2+} compared with that at 10 nM Ca^{2+}. IP_3 concentrations were 0.3 μM for cells expressing subtype(s) 2, 1/2, 2/3, 1/2/3; 6 μM for subtype(s) 1, 1/3; and 20 μM for subtype 3. Ca^{2+} release via IP_3R-1 was studied in the presence of 5 mM ATP. Results are the mean ± SEM for 3–5 experiments.

underlie the regenerative Ca^{2+} release during the Ca^{2+} wave and rapid upstroke of $[Ca^{2+}]_i$ increase (Iino and Endo, 1992; Lechleiter and Clapham, 1992; Iino *et al*., 1993; Bootman *et al*., 1997; Horne and Meyer, 1997). Ca^{2+} release via IP_3R-1 and IP_3R-2 exhibited clear biphasic Ca^{2+} dependence with a peak rate obtained near 300 nM (Figure 6A), whereas IP_3R-3-mediated Ca^{2+} release exhibited flatter Ca^{2+} dependence. Figure 6C plots the extent of Ca^{2+}-induced activation, or the percentage activation of the rate of Ca^{2+} release, when the cytoplasmic Ca^{2+} concentration was increased from 10 to 300 nM in cells containing the various IP_3R subtypes.

Functional interaction between IP_3R subtypes

It has been shown that the IP_3R subtypes form hetero-tetramers (Joseph *et al*., 1995; Monkawa *et al*., 1995), which were thought to create an additional degree of variability with regard to the IP_3R function. However, functional interactions between the IP_3R subtypes have not previously been investigated. We studied IP_3-induced Ca^{2+} release in cells expressing multiple IP_3R subtypes. The IP_3 dependence of the Ca^{2+} release rate in cells with multiple IP_3R subtypes was closely fitted by the summation of the fits to the corresponding individual subtypes after reduction of the maximal rates to 31–82% of those in cells expressing a single subtype (Figure 5B, dotted curves). The downward scaling of the maximal release rate may reflect compensatory upregulation of IP_3Rs in cells expressing only a single subtype. This is consistent with the increased mRNA or protein levels observed in mutant cells (Figure 1). We also studied the ATP and Ca^{2+} dependence of Ca^{2+} release in cells expressing multiple subtypes (Figures 4C and 6B). When IP_3R-1 and IP_3R-3 were coexpressed, the ATP dependence was similar

to that of IP_3R-3 but the Ca^{2+} dependence was similar to that of IP_3R-1. IP_3-induced Ca^{2+} release in cells expressing both IP_3R-1 and IP_3R-2 lost the prominent ATP dependence that was characteristic of IP_3R-1. Cells expressing both IP_3R-2 and IP_3R-3 showed ATP and Ca^{2+} sensitivities similar to those of IP_3R-2-expressing cells. In wild-type cells, the ATP sensitivity was similar to that of IP_3R-2-expressing cells. Taken together, coexpression of multiple subtypes resulted in simple additive IP_3 sensitivity, whereas the property of either one of the subtypes became dominant in terms of ATP and Ca^{2+} sensitivity. The latter result indicates that there is indeed a molecular interaction between the different subtypes, probably within the hetero-tetrameric structure of the Ca^{2+} release channels.

Ca^{2+} signalling and IP_3R subtypes

The present results highlight the functional variations among IP_3R subtypes. IP_3R-1, when expressed singly, exhibited prominent ATP dependence and the potential to function as an ATP sensor just like the ATP-sensitive K^+ channels in pancreatic β cells. IP_3R-3 has the lowest IP_3 and Ca^{2+} sensitivities, while IP_3R-2 has the highest sensitivity to IP_3. The order of IP_3 sensitivity is in general agreement with that of the IP_3-binding affinity of the IP_3R subtypes (Newton *et al*., 1994). Furthermore, BCR-mediated Ca^{2+}-signalling patterns differed significantly among cells expressing different IP_3R subtypes: Ca^{2+} oscillations were found in IP_3R-1 and -2 expressing cells, while monophasic Ca^{2+} transients were observed in IP_3R-3-expressing cells. Although difference in the level of expression of various IP_3R subtypes may affect the Ca^{2+}-signalling patterns, the following considerations make it unlikely to be a major determinant in the present study. The expression levels of IP_3R subtypes can be estimated from r_{max}, i.e. the maximum rate of Ca^{2+} release, and the values were comparable within a factor of two among DT40 clones expressing different IP_3R subtypes (Figure 5A). If we take ATP dependence of IP_3R-3 into consideration (see Figure 4C), difference in r_{max} values between IP_3R-2- and IP_3R-3-expressing cells is probably minimal under physiological intracellular conditions, where ATP is present at millimolar levels. Moreover, the r_{max} value of IP_3R-3-expressing cells was greater than that of IP_3R-1-expressing cells even in the presence of ATP. Thus there is no correlation between the Ca^{2+}-oscillation pattern in intact cells and the level of functional expression of IP_3Rs.

We have obtained evidence for the first time that coexpressed IP_3R subtypes interact functionally. Co-expression of subtypes with different affinities for IP_3 widens the range of IP_3 sensitivity of intracellular Ca^{2+} stores. Furthermore, expression of IP_3R-2, with or without other subtypes, facilitates Ca^{2+} oscillations in DT40 cells. It is of interest to note that IP_3R-2 is the dominantly expressed IP_3R in hepatocytes (Wojcikiewicz *et al*., 1994), in which Ca^{2+} oscillations were first observed (Woods *et al*., 1986). The high IP_3 sensitivity of IP_3R-2 may underlie the long-lasting Ca^{2+} oscillations, but other possibilities, such as preferential modification of IP_3R-2 during Ca^{2+} oscillations, cannot be excluded. The expression patterns of IP_3R subtypes differ among different tissues (Newton *et al*., 1994; Wojcikiewicz *et al*., 1994), during development (Dent *et al*., 1996), and in subcellular localization (Lee *et al*., 1997). Our results provide a clear functional basis for the physiological significance of the differential expression of IP_3R subtypes in cell-type-specific encoding of Ca^{2+} signalling.

Materials and methods

Cell culture and generation of DT40 B cells expressing only IP_3R-1 or IP_3R-2

DT40 chicken B lymphoma cells were cultured in RPMI1640 supplemented with 10% fetal calf serum (FCS), 1% chicken serum, penicillin, streptomycin and glutamine. To inactivate the IP_3R-3 gene, two targeting vectors, pIP_3R type 3-*bleo* and pIP_3R type 3-*bsr*, were used. The latter was constructed by replacing the *bleo* cassette of pIP_3R type 3-*bleo* (Sugawara *et al*., 1997) with the *bsr* cassette. For disruption of both alleles of the IP_3R-3 gene, these two targeting vectors were transfected sequentially into DT40 cells expressing a combination of IP_3R-1/IP_3R-3 or IP_3R-2/IP_3R-3, thereby resulting in the generation of DT40 cells expressing only IP_3R-1 or IP_3R-2, respectively. Other IP_3R gene-targeted DT40 cells had been established previously (Sugawara *et al*., 1997).

Northern analysis

RNA was prepared from wild-type and mutant DT40 cells using the guanidium thiocyanate method. Total RNA (20 μg) was separated in a 1.2% formaldehyde gel, transferred onto a Hybond-N membrane and probed with ^{32}P-labelled cDNA fragments specific for each type of chicken IP_3R gene (Sugawara *et al*., 1997) and the chicken β-actin gene (Kost *et al*., 1983).

Immunoprecipitation and immunoblotting

Cells were lysed in a solution containing 30 mM Tris–HCl pH 8.0, 10 mM EDTA, 0.1% SDS, 0.5% sodium deoxycholate, 1% NP-40, 1 mM Na_3VO_4, 30 mM NaF, 1 mM PMSF, 10 μg/ml leupeptin, 10 μg/ml aprotinin and 0.1% bovine serum albumen (BSA) (lysis buffer). Lysates were clarified by centrifugation at 15 000 *g* for 10 min at 4°C. Immunoprecipitation was performed at 4°C using a rabbit polyclonal anti-IP_3R antibody (raised against a synthetic peptide within the C-terminal cytoplasmic domain of either chicken IP_3R-1, LGHPPPMNVPQPA, or IP_3R-2, LGSHTPHVNHHMPPP) for >1 h, and then with addition of protein G–Sepharose for >1 h. The immune complexes were washed and heated at 100°C in SDS sample buffer. Solubilized proteins were separated by SDS–PAGE and transferred electrophoretically to a PVDF membrane. After blocking in 5% fatty acid-free BSA, the blot was incubated with the same anti-IP_3R antibody and then incubated with [^{125}I]protein G. The associated radioactivity was visualized using a Fuji BAS2000 Bio Imaging Analyzer.

Ca^{2+} imaging

Cells were attached to poly-L-lysine and collagen-coated coverslips, and loaded with either 1 μM Fura-2AM for 20–30 min or 20 μM FuraptraAM for 60 min in a physiological salt solution: 150 mM NaCl, 4 mM KCl, 2 mM $CaCl_2$, 1 mM $MgCl_2$, 5 mM HEPES, 5.6 mM glucose, pH 7.4. The Furaptra-loaded cells were then permeabilized by incubation with 40 μM β-escin for 2–4 min in an internal solution (Hirose *et al*., 1998) to wash out the Furaptra in the cytoplasm, which enabled measurement of the Ca^{2+} concentration within the organelles. An Olympus IX70 inverted microscope, equipped with a cooled CCD camera (Photometrics, USA) and a polychromatic illumination system (T.I.L.L. Photonics, Germany), was used to capture the fluorescence images at a rate of one pair of frames with excitations at 340 and 380 nm per 1, 2, 5 or 10 s. The ratio of the fluorescence intensity between the pair of frames was then calculated after subtraction of the baseline fluorescence. Cells were viewed under an oil-immersion objective (100×, NA 1.35). Experiments were carried out at room temperature (22–24°C), and solutions were applied to the cells through an electrically controlled puffing pipette. Solutions containing various concentrations of Ca^{2+} were prepared by mixing CaEGTA and EGTA solutions at appropriate ratios (Hirose *et al*., 1998).

Evaluation of IP_3R activity

The IP_3R activity was evaluated in terms of the initial Ca^{2+} release rate as described previously (Hirose and Iino, 1994). Briefly, the observed change in the ratio of fluorescence intensities of 30–40 cells within a frame were normalized so that 1 and 0 corresponded, respectively, to the values just before the application of IP_3 and after complete depletion

by 10 μM IP_3 at 300 nM Ca^{2+}. The initial 20 s period of the normalized time course was fitted by a single exponential function, e^{-rt}. The rate constant, r (s^{-1}), thus estimated was used as an index of the IP_3R activity.

Acknowledgements

The authors thank Dr Mari Kurosaki for help at various stages of the work and Izumi Shibata for technical assistance. This work was partly supported by grants from the Ministry of Education, Science, Sport and Culture of Japan.

References

Berridge,M.J. (1993) Inositol trisphosphate and calcium signalling. *Nature*, **361**, 315–325.

Bezprozvanny,I. and Ehrlich,B. (1993) ATP modulates the function of inositol 1,4,5-trisphosphate-gated channels at two sites. *Neuron*, **10**, 1175–1184.

Bezprozvanny,I., Watras,J. and Ehrlich,B.E. (1991) Bell-shaped calcium-response curve of Ins (1,4,5)P_3- and calcium-gated channels from endoplasmic reticulum of cerebellum. *Nature*, **351**, 751–754.

Bootman,M.D., Berridge,M.J. and Lipp,P. (1997) Cooking with calcium: the recipes for composing global signals from elementary events. *Cell*, **91**, 367–373.

De Koninck,P. and Schulman,H. (1998) Sensitivity of CaM kinase II to the frequency of Ca^{2+} oscillations. *Science*, **279**, 227–230.

Dent,M.A., Raisman,G. and Lai,F.A. (1996) Expression of type 1 inositol 1,4,5-trisphosphate receptor during axogenesis and synaptic contact in the central and peripheral nervous system of developing rat. *Development*, **122**, 1029–1039.

Dolmetsch,R.E., Xu,K. and Lewis,R.S. (1998) Calcium oscillations increase the efficiency and specificity of gene expression. *Nature*, **392**, 933–936.

Finch,E.A., Turner,T.J. and Goldin,S.M. (1991) Calcium as a coagonist of inositol 1,4,5-trisphosphate-induced calcium release. *Science*, **252**, 443–446.

Hagar,R.E., Burgstahler,A.D., Natanson,M.H. and Ehrlich,B.E. (1998) Type III $InsP_3$ receptor channel stays open in the presence of increased calcium. *Nature*, **396**, 81–84.

Hajnóczky,G. and Thomas,A.P. (1997) Minimal requirements for calcium oscillations driven by the IP_3 receptor. *EMBO J.*, **16**, 3533–3543.

Hirose,K. and Iino,M. (1994) Heterogeneity of channel density in inositol 1,4,5-trisphosphate-sensitive Ca^{2+} stores. *Nature*, **372**, 791–794.

Hirose,K., Kadowaki,S. and Iino,M. (1998) Allosteric regulation by cytoplasmic Ca^{2+} and IP_3 of the gating of IP_3 receptors in permeabilized guinea-pig vascular smooth muscle cells. *J. Physiol.*, **506**, 407–414.

Hofer,A.M. and Machen,T.E. (1993) Technique for *in situ* measurement of calcium in intracellular inositol 1,4,5-trisphosphate-sensitive stores using the fluorescent indicator mag-fura-2. *Proc. Natl Acad. Sci. USA*, **90**, 2598–2602.

Horne,J.H. and Meyer,T. (1997) Elementary calcium-release units induced by inositol trisphosphate. *Science*, **276**, 1690–1693.

Iino,M. (1990) Biphasic Ca^{2+} dependence of inositol 1,4,5-trisphosphate-induced Ca release in smooth muscle cells of the guinea pig taenia caeci. *J. Gen. Physiol.*, **95**, 1103–1122.

Iino,M. (1991) Effects of adenine nucleotides on inositol 1,4,5-trisphosphate-induced calcium release in vascular smooth muscle cells. *J. Gen. Physiol.*, **98**, 681–698.

Iino,M. and Endo,M. (1992) Calcium-dependent immediate feedback control of inositol 1,4,5-trisphosphate-induced Ca^{2+} release. *Nature*, **360**, 76–78.

Iino,M., Yamazawa,T., Miyashita,Y., Endo,M. and Kasai,H. (1993) Critical intracellular Ca^{2+} concentration for all-or-none Ca^{2+} spiking in single smooth muscle cells. *EMBO J.*, **12**, 5287–5291.

Joseph,S.K., Lin,C., Pierson,S., Thomas,A.P. and Maranto,A.R. (1995) Heteroligomers of type-I and type-III inositol trisphosphate receptors in WB rat liver epithelial cells. *J. Biol. Chem.*, **270**, 23310–23316.

Kost,T.A., Theodorakis,N. and Hughes,S.H. (1983) The nucleotide sequence of the chick cytoplasmic β-actin gene. *Nucleic Acids Res.*, **11**, 8287–8301.

Kurosaki,T. (1997) Molecular mechanisms in B cell antigen receptor signaling. *Curr. Opin. Immunol.*, **9**, 309–318.

Lechleiter,J.D. and Clapham,D.E. (1992) Molecular mechanisms of intracellular calcium excitability in *X. laevis* oocytes. *Cell*, **69**, 283–294.

Lee,M.G., Xu,X., Zeng,W., Diaz,J., Wojcikiewicz,R.J., Kuo,T.H., Wuytack,F., Racymaekers,L. and Muallem,S. (1997) Polarized expression of Ca^{2+} channels in pancreatic and salivary gland cells. Correlation with initiation and propagation of $[Ca^{2+}]_i$ waves. *J. Biol. Chem.*, **272**, 15765–15770.

Li,W., Llopis,J., Whitney,M., Zlokarnik,G. and Tsien,R.Y. (1998) Cell-permeant caged $InsP_3$ ester shows that Ca^{2+} spike frequency can optimize gene expression. *Nature*, **392**, 936–941.

Missiaen,L., Parys,J.B., Sienaert,I., Maes,K., Kunzelmann,K., Takahashi,M., Tanzawa,K. and De Smedt,H. (1998) Functional properties of the type-3 $InsP_3$ receptor in 16HBE14o–bronchial mucosal cells. *J. Biol. Chem.*, **273**, 8983–8986.

Monkawa,T., Miyawaki,A., Sugiyama,T., Yoneshima,H., Yamamoto-Hino,M., Furuichi,T., Saruta,T., Hasegawa,M. and Mikoshiba,K. (1995) Heterotetrameric complex formation of inositol 1,4,5-trisphosphate receptor subunits. *J. Biol. Chem.*, **270**, 14700–14704.

Newton,C.L., Mignery,G.A. and Südhof,T.C. (1994) Co-expression in vertebrate tissues and cell lines of multiple inositol 1,4,5-trisphosphate ($InsP_3$) receptors with distinct affinities for $InsP_3$. *J. Biol. Chem.*, **269**, 28613–28619.

Raju,B., Murphy,E., Levy,L.A., Hall,R.D. and London,R.E. (1989) A fluorescent indicator for measuring cytosolic free magnesium. *Am. J. Physiol.*, **256**, C540–C548.

Ramos-Franco,J., Fill,M. and Mignery,G.A. (1998) Isoform-specific function of single inositol 1,4,5-trisphosphate receptor channels. *Biophys. J.*, **75**, 834–839.

Sugawara,H., Kurosaki,M., Takata,M. and Kurosaki,T. (1997) Genetic evidence for involvement of type 1, type 2 and type 3 inositol 1,4,5-trisphosphate receptors in signal transduction through the B-cell antigen receptor. *EMBO J.*, **16**, 3078–3088.

Wojcikiewicz,R.J. (1995) Type I, II and III inositol 1,4,5-trisphosphate receptors are unequally susceptible to down-regulation and are expressed in markedly different proportions in different cell types. *J. Biol. Chem.*, **270**, 11678–11683.

Wojcikiewicz,R.J., Furuichi,T., Nakade,S., Mikoshiba,K. and Nahorski,S.R. (1994) Muscarinic receptor activation down-regulates the type I inositol 1,4,5-trisphosphate receptor by accelerating its degradation. *J. Biol. Chem.*, **269**, 7963–7969.

Woods,N.M., Cuthbertson,K.S.R. and Cobbold,P.H. (1986) Repetitive transient rises in cytoplasmic free calcium in hormone-stimulated hepatocytes. *Nature*, **319**, 600–602.

Received July 2, 1998; revised December 12, 1998; accepted January 12, 1999